Polyhedron 31 (2012) 202–209

Contents lists available at SciVerse ScienceDirect

Polyhedron

journal homepage: www.elsevier.com/locate/poly

Synthesis, characterization and molecular structures of barium(II) trichloroacetate DME/1,4-dioxane compounds

Sukhjinder Singh [a,*], Deepika Saini [a], S.K. Mehta [a], Ravneet Kaur [a], Valeria Ferretti [b,*]

[a] Department of Chemistry and Centre of Advanced Studies in Chemistry, Panjab University, Chandigarh 160 014, India
[b] Centro di Strutturistica Diffrattometrica and Dipartimento di Chimica, University of Ferrara, Via L. Borsari 46, I-44121 Ferrara, Italy

ARTICLE INFO

Article history:
Received 26 May 2011
Accepted 11 September 2011
Available online 21 September 2011

Keywords:
Trichloroacetates
DME
1,4-Dioxane
Barium
X-ray structure

ABSTRACT

Two new barium(II) trichloroacetate compounds, $[Ba(H_2O)(DME)(\mu\text{-}O_2CCCl_3)_2]_n$ (**1**) and $[\{Ba(H_2O)_2(diox)_{0.5}(\mu\text{-}O_2CCCl_3)_2\}(diox)]_n$ (**2**) were synthesized and characterized by elemental analyses, physiochemical studies, FT-IR, ^1H NMR, thermogravimetric analyses (TG/DTG/DSC) and single crystal X-ray studies. The reaction of hydrated barium(II) trichloroacetate monohydrate with excess DME (1,2-dimethoxyethane) and diox (1,4-dioxane) in methanol at room temperature led to the isolation of the novel compounds **1** and **2**, respectively. Bridging trichloroacetate groups are anticipated on the basis of FT-IR studies and this was confirmed by the X-ray studies. Both compounds dissociate to produce ions in water, as shown by molar conductance values. ^1H NMR spectroscopy confirms that DME and 1,4-dioxane are coordinated to the metal ion in these compounds. Single crystal X-ray diffraction studies reveal that the barium cation is coordinated to nine O atoms in a deformed coordination polyhedron in both compounds. Structural data of barium(II) trichloroacetates compounds have been obtained for the first time in the present investigation.

1. Introduction

Supramolecular and coordination chemistry have provided important advances in developing strategies for the synthesis of complex molecular architectures and novel assemblies [1–3]. Alkaline earth metal compounds [4–9] have attracted a lot of attention because of their widespread use in a number of advanced material applications [10–13]. Increasing interest in the search for alkaline earth molecular precursors for the generation of high temperature superconductors, ceramics and nano materials have led to the isolation of a variety of alkaline earth metal zero-dimensional, low-dimensional, three dimensional coordination polymer networks and heterometallic compounds [14–22]. Especially, barium precursors have played a significant role in the development of property controlled thin films for ceramic $YBa_2Cu_3O_{7-\delta}$ (YBCO) superconductor materials [10,11]. Alkaline earth metal alkoxides [23,24] and β-diketonates [25–28] are very promising as Metal Organic Chemical Vapor Deposition (MOCVD) precursors for metal oxide superconductors. In general, metal alkoxides $M(OR)_x$ are excellent precursors for the production of ceramic materials [12,29–34], however the low solubility and high crystallization temperature of $Ba(OR)_2$ deters its use for the development of YBCO materials [10,11,35–37]. The high volatility of soluble acetylacetonate precursors often results in a change in the stoichiometry of the final films [10,11,35–37] which restricts their use. The use of simple carboxylates also suffers from decomposition pathways that proceed via carbonate intermediates during processing [10,11,35–37]. In this context, highly halogenated derivatives of carboxylic acid (e.g. trifluoroacetates/trichloroacetates) may prove extremely useful because of the solubility, volatility and carbonate problems [38,39]. The preferential decomposition of barium fluoroacetates into barium fluoride [40] represents a means to avoid the formation of the highly stable carbonate, which is detrimental to the superconducting properties.

On the other hand, large numbers of crystallographic structural reports of various metal trichloroacetates are available in the literature, with the trichloroacetate ligand (TCLA) adopting numerous binding modes such as unidentate, bidentate chelating and bidentate bridging. However, only few hetero-metallic alkaline earth metal trichloroacetates have been structurally characterized [41,42]. Therefore, we undertook the synthesis of new barium(II) trichloroacetate compounds, viz $[Ba(H_2O)(DME)(\mu\text{-}O_2CCCl_3)_2]_n$ (**1**) and $[\{Ba(H_2O)_2(diox)_{0.5}(\mu\text{-}O_2CCCl_3)_2\}(diox)]_n$ (**2**) [DME = 1,2-dimethoxyethane and diox = 1,4-dioxane] and their characterization by elemental analysis, molar conductance, IR, ^1H NMR and thermogravimetric analysis (TG/DTG/DSC). To the best of our knowledge we are reporting the single crystal structures of barium TCLA compounds **1** and **2** for the first time.

* Corresponding authors. Tel.: +91 0172 2534429; fax: +91 0172 2545074 (S. Singh), tel.: +39 0532 455132/455144; fax: +39 0532 240709 (V. Ferretti).
E-mail addresses: sukhis@pu.ac.in (S. Singh), frt@unife.it (V. Ferretti).

0277-5387/$ - see front matter © 2011 Elsevier Ltd. All rights reserved.
doi:10.1016/j.poly.2011.09.018

2. Experimental

2.1. Materials

Commercially available analytical grade reagents [1,4-dioxane (diox), 1,2-dimethoxyethane (DME), methanol] were used throughout this work without further purification. Trichloroacetic acid (Merck) and barium(II) carbonate (BDH) were used as received.

2.2. Physical measurements

Carbon and hydrogen were determined microanalytically using an automatic Perkin-Elmer 2400 CHN/Analytischer Funktionstest vario EL II Fab. Nr. 11975059 elemental analyzer. Barium and chlorine were determined gravimetrically by standard literature methods [43]. Infrared spectra were recorded as KBr pellets on a Perkin-Elmer RXFT-IR spectrophotometer in the region 4000–400 cm^{-1}. Conductance measurements were performed on a Pico conductivity meter (Model CNO4091201, Lab India) at 25 °C. The thermogravimetric analyses were carried out in a dynamic nitrogen atmosphere (100 mL min^{-1}) at the heating rate of 10 °C min^{-1} using a Universal V4 SDT Q-600 V20.9 thermal analyzer. Simultaneous TG–DTG–DSC curves as well as separate TG curves were obtained. ^1H NMR spectra were recorded in D_2O at ambient temperature on a Bruker Avance II 400 MHz NMR spectrometer. Tetramethylsilane (TMS) was used as an external standard for the ^1H NMR spectra.

2.3. Synthesis

2.3.1. $Ba(O_2CCCl_3)_2{\cdot}H_2O$

Excess $BaCO_3$ (4.54 g, 23.05 mmol) was added to a solution of trichloroacetic acid (5.98 g, 36.57 mmol) in 30 mL of water. The contents were stirred at room temperature until the evolution of CO_2 ceased. Excess $BaCO_3$ was then filtered off. Removal of solvent from the filtrate under vacuum gave 8.69 g (18.10 mmol) of white shining crystalline $Ba(O_2CCCl_3)_2{\cdot}H_2O$ in nearly quantitative yield (99%). *Anal.* Calc. for $C_4H_2BaCl_6O_5$: C, 10.00; H, 0.42; Cl, 44.37; Ba, 28.54. Found: C, 10.15; H, 0.43; Cl, 43.95; Ba, 28.12%. FT-IR (KBr pellets, cm^{-1}): 3393 sbr (OH stretch.); 1642 s (COO asym. stretch.); 1351 ms (COO sym. stretch.); 952 w (C–C stretch.); 844 s (CCl_3 asym. stretch.); 756 ms; 745 m; 681 s (where br = broad; m = medium; s = strong; v = very; w = weak; sh = shoulder). M.pt. >54 °C (decomp.).

2.3.2. $[Ba(H_2O)(DME)(\mu\text{-}O_2CCCl_3)_2]_n$ (**1**)

The present compound was prepared by the slow addition of 5 mL of DME (1,2-dimethoxyethane) to a solution of $Ba(O_2CCCl_3)_2{\cdot}H_2O$ (2.04 g, 4.25 mmol) in 25 mL of methanol with constant stirring. The white shining crystals of **1** 1.67 g (2.93 mmol) suitable for X-ray diffraction were obtained in 68.9% yield over a period of 3 days by slow evaporation of solvent at room temperature. *Anal.* Calc. for $C_8H_{12}BaCl_6O_7$: C, 16.83; H, 2.10; Cl, 37.35; Ba, 24.08. Found: C, 16.81; H, 1.98; Cl, 37.02; Ba, 24.11%. FT-IR (KBr pellets, cm^{-1}): 3672 w, 3391 mbr (OH stretch.); 3008 vw, 2937 vw, 2832 vw (C–H stretch.); 1678 m, 1648 s (COO asym. stretch.); 1380 sh, 1355 s (COO sym. stretch.); 951 vw (C–C asym. stretch.); 875 sh, 841 vs (CCl_3 asym. stretch.); 567 wb (M–O vib.); 1617 sh; 1452 vw; 1329 mw; 1248 vw; 1193 vw; 1119 w; 1069 ms; 1028 vw; 749 s; 681 vs; 452 w (cm^{-1}). ^1H NMR (400 MHz, D_2O) δ (ppm): 3.28 (s, 6H, 2-OCH_3), 3.51 (s, 4H, $2CH_2$). M.pt. >62 °C (decomp.).

2.3.3. $[\{Ba(H_2O)_2(diox)_{0.5}(\mu\text{-}O_2CCCl_3)_2\}(diox)]_n$ (**2**)

Dioxane was added slowly to a solution of $Ba(O_2CCCl_3)_2{\cdot}H_2O$ (1.73 g, 3.6 mmol) in 20 mL of methanol until white precipitates appeared. The precipitates were redissolved by adding methanol and the resulting clear solution was stirred at room temperature for 1 h. About 1.56 g (2.48 mmol) of **2** as white shining transparent needle-shaped crystals, suitable for X-ray diffraction, were obtained in 68.9% yield over a period of 4 days via slow evaporation of solvent at room temperature. *Anal.* calc. for $C_{10}H_{16}BaCl_6O_9$: C, 19.05; H, 2.54; Cl, 33.81; Ba, 21.74. Found: C, 18.83; H, 2.51; Cl, 32.94; Ba, 21.25%. FT-IR (KBr pellets, cm^{-1}): 3505 mw, 3422 m (O–H stretch.); 2968 w, 2923 mw, 2865 w (C–H stretch.); 1661 vsb (COO asym. stretch.); 1378 m, 1347 s (COO sym. stretch.); 942 vw (C–C stretch.); 874 ms, 833 sb (CCl_3 asym. stretch.); 614 mw (M–O vib.); 1454 w; 1293 w; 1256 m; 1115 ms; 1080 mw; 1045 vw; 890 mw; 751 ms; 684 ms; 428 wb. ^1H NMR (400 MHz, D_2O) δ (ppm): 3.63 (s, 8H, $4CH_2$). M.Pt. >85 °C (decomp.).

2.3.4. X-ray crystal structure information

The crystallographic data for **1** and **2** were collected on a Nonius Kappa CCD diffractometer at room temperature using graphite-monochromated Mo Kα radiation (λ = 0.71073 Å). Data sets were integrated with the Denzo-SMN package [44] and corrected for Lorentz-polarization and absorption effects [45]. The crystal parameters and other experimental details of the data collections are summarized in Table 1. The structures were solved by direct methods (SIR97) [46] and refined by full-matrix least-squares methods with all non-hydrogen atoms as anisotropic. Hydrogens were included in calculated positions, riding on their carrier atoms, apart from those belonging to water molecules that were located in the difference-fourier map. Cl2–Cl6 atoms in **1** were found to be disordered over two equivalent positions. All calculations were performed using SHELXL-97 [47] implemented in the WINGX system of programs [48]. Selected bond distances and angles are given in Table 2.

3. Results and discussion

3.1. Synthesis and characterization

The reaction between trichloroacetic acid and excess $BaCO_3$ in aqueous medium at room temperature resulted in the formation of $Ba(O_2CCCl_3)_2{\cdot}H_2O$ as is given below:

$$BaCO_3 + 2CCl_3COOH \xrightarrow[R.T.]{H_2O} Ba(O_2CCCl_3)_2 \cdot H_2O + CO_2$$

Table 1
Experimental details.

	Compound **1**	Compound **2**
M_r	561.21	630.27
Crystal system	monoclinic	triclinic
Space group	$C2/c$	$P\bar{1}$
a (Å)	21.3473 (6)	8.8379 (1)
b (Å)	12.3488 (4)	10.8247 (2)
c (Å)	15.0432 (5)	12.3044 (3)
α (°)	90	99.2990 (8)
β (°)	97.7510 (11)	99.4480 (8)
γ (°)	90	104.3970 (9)
V (Å^3)	3929.4 (2)	1099.17 (4)
Z	8	2
μ (mm^{-1})	2.86	2.57
Crystal size (mm)	0.43 × 0.17 × 0.14	0.29 × 0.17 × 0.12
No. of measured, independent and observed [$I > 2\sigma(I)$] reflections	13 736, 4695, 3896	22 038, 6363, 5051
R_{int}	0.047	0.074
$R[F^2 > 2\sigma(F^2)]$	0.045	0.042
$wR(F^2)$	0.121	0.105
S	1.10	1.08
No. of reflections	4695	6363
No. of parameters	245	241
$\Delta\rho_{max}$, $\Delta\rho_{min}$ (e Å^{-3})	1.40, −2.12	0.74, −1.70

Table 2
Selected bond distances and angles (Å, °).

Compound ***1***			
Ba1–O1	2.952(3)	Ba1–O5	2.867(5)
Ba1–O2	2.872(4)	Ba1–O6	2.835(4)
Ba1–O3	2.719(3)	Ba1–O7	2.902(3)
Ba1–O2′ (−*x*, *y*, 1/2 − *z*)	2.802(3)		
Ba1–O1″ (−*x*, −*y*, −*z*)	2.734(3)		
Ba1–O4″ (−*x*, −*y*, −*z*)	2.729(4)		
O1–Ba1–O3	70.0(1)	O2–Ba1–O6	146.6(1)
O1–Ba1–O5	150.5(1)	O3–Ba1–O5	134.2(1)
O1–Ba1–O6	148.6(1)	O3–Ba1–O6	78.6(1)
O1–Ba1–O7	98.9(1)	O3–Ba1–O7	156.2(1)
O2–Ba1–O5	127.5(1)	O5–Ba1–O6	57.7(1)
O2–Ba1–O3	96.2(1)	O5–Ba1–O7	64.1(1)
O2–Ba1–O7	63.48(7)	O6–Ba1–O7	111.1(1)
Compound ***2***			
Ba1–O1	2.874(3)	Ba1–O5	3.018(3)
Ba1–O2	2.775(3)	Ba1–O1W	2.784(3)
Ba1–O3	3.136(3)	Ba1–O2W	2.768(3)
Ba1–O4	2.817(3)		
Ba1–O5′ (−*x*, 1 − *y*, −*z*)	2.760(3)		
Ba1–O3″ (1 − *x*, 1 − *y*, −*z*)	2.729(3)		
O1–Ba1–O2	143.08(9)	O3–Ba1–O4	71.38(8)
O1–Ba1–O4	131.91(9)	O3–Ba1–O5	89.58(8)
O1–Ba1–O5	143.73(8)	O3–Ba1–O2W	153.60(8)
O1–Ba1–O1W	71.3(1)	O4–Ba1–O1W	133.33(9)
O1–Ba1–O2W	72.91(9)	O4–Ba1–O2W	82.22(9)
O2–Ba1–O4	82.3(1)	O5–Ba1–O1W	142.31(9)
O2–Ba1–O1W	74.1(1)	O1W–Ba1–O2W	141.55(9)
O2–Ba1–O2W	134.59(9)		

The use of excess $BaCO_3$ helps in the complete consumption of trichloroacetic acid. The white crystalline $Ba(O_2CCCl_3)_2{\cdot}H_2O$ is soluble in water and alcohols. Anhydrous barium(II) trichloroacetate and hydrated barium(II) trichloroacetate (the number of water molecules is not defined) are known [49,50]. However, barium(II) trichloroacetate monohydrate is not known. Further reaction of DME or 1,4-dioxane with $Ba(O_2CCCl_3)_2{\cdot}H_2O$ in methanol led to the isolation of novel compounds **1** and **2**, respectively, as outlined below:

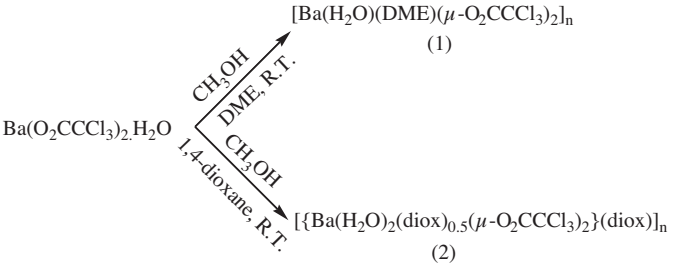

The isolated white crystalline new compounds **1** and **2** are soluble in a number of solvents, e.g. THF, alcohols, H_2O, nitromethane, DMSO/DMF etc. The composition of compound **2**, i.e. $[\{Ba(H_2O)_2(diox)_{0.5}(\mu\text{-}O_2CCCl_3)_2\}(diox)]_n$ having two moles of water, has been accomplished by absorbing water from the solvent (CH_3OH as well as 1,4-dioxane) since both solvents were not dried before use.

3.2. Spectroscopic characterization

The FT-IR spectral data of the starting compound $Ba(O_2CCCl_3)_2{\cdot}H_2O$ and both compounds **1** and **2**, recorded as KBr pellets, are given in Section 2. The crystal structures of anhydrous and hydrated barium(II) trichloroacetates are unknown. However, IR spectral data of hydrated barium(II) trichloroacetate has been reported in the literature [50]. The band at 3393 cm^{-1} in $Ba(O_2CCCl_3)_2{\cdot}H_2O$ is assigned to O–H stretching vibrations of the water of crystallization, similar to the reported band at 3540 cm^{-1} in the IR spectrum of hydrated barium(II) trichloroacetate [50]. The bands at 1642 and 1351 cm^{-1} in the starting compound $Ba(O_2CCCl_3)_2{\cdot}H_2O$ are assigned to the asymmetric and symmetric COO stretching vibrations, respectively, similar to the bands at 1670 (COO asymmetric stretch.) and 1379 (COO symmetric stretch.) cm^{-1} in hydrated barium(II) trichloroacetate [50]. The bands at 3672, 3391 and 3505, 3422 cm^{-1} in **1** and **2**, respectively, may be attributed to OH stretching vibrations of water. The C–H stretching vibrations are observed as weak absorptions in the 2830–3008 cm^{-1} region in both compounds. A very strong absorption at 1648 cm^{-1} and a weak peak at 1678 cm^{-1} in **1** may be attributed to COO asymmetric stretching vibrations of the unsymmetrical trichloroacetate ligands. The strong band at 1355 cm^{-1} with a shoulder at 1380 cm^{-1} in **1** may be assigned to the corresponding COO symmetric stretching vibrations of the respective CCl_3CO_2 groups. Thus, the magnitude of Δ (COO asymmetric stretch – COO symmetric stretch), of the order of 293 (=1648–1355) cm^{-1}, suggests bidentate bridging trichloroacetate groups in **1**. Similar results have also been observed in the case of metal trichloroacetates [51–53] and other metal carboxylates [54,55]. A very strong band at 841 cm^{-1} with a shoulder at 875 cm^{-1} in **1** is assigned to the C–Cl stretching vibrations of the CCl_3COO groups. A very strong broad absorption band at 1661 cm^{-1} in **2** may be attributed to the COO asymmetric stretching vibrations of the trichloroacetate ligands, and two bands at 1378 and 1347 cm^{-1} in **2** may be attributed to COO symmetric stretching vibrations of unsymmetrical CCl_3COO groups. Again, the magnitude of Δ (COO asymmetric stretch – COO symmetric stretch), of the order of 283 (=1661–1378) cm^{-1}, indicates bidentate bridging trichloroacetate ligands in **2**. The splitting of the COO stretching modes in compounds **1** and **2**, as compared to the respective single peaks in the starting compound $Ba(O_2CCCl_3)_2{\cdot}H_2O$, suggests a different environment of the CCl_3COO ligands around the metal ion in compounds **1** and **2**, in contrast to $Ba(O_2CCCl_3)_2{\cdot}H_2O$. The bands at 874 and 833 cm^{-1} in **2** may be ascribed to C–Cl stretching vibrations of the trichloroacetate ligands. The weak absorption at 567 cm^{-1} in **1** and at 614 cm^{-1} in **2** may be attributed to M–O vibrations.

^1H NMR spectra of **1** and **2** were recorded in D_2O. Two sharp singlets were observed at 3.28 and 3.51 ppm relative to TMS due to two $-OCH_3$ and two $-CH_2-$ groups, respectively, of DME ($CH_3OCH_2CH_2OCH_3$) in compound **1**. The downfield values observed in compound **1** relative to that of pure DME (3.16 and 3.35 ppm) indicate chelation of DME to the metal. In compound **2**, a sharp singlet at 3.63 ppm was observed due to the CH_2 groups of 1,4-dioxane.

3.3. Molar conductance

Conductance measurements of **1** and **2** were carried out at 25 °C in water. The extrapolation of $\sqrt{C}$ to zero for both the compounds gave values of Λ_m of the order of 190.2 for **1** and 203 S cm^2 mol^{-1} for **2**. These values are fairly close to the expected range for a 1:2 electrolyte [56]. Conductance measurements, therefore, reveal that the complexes dissociate to produce ions in aqueous media.

3.4. X-ray studies

ORTEPIII [57] views of compounds **1** and **2** are shown in Fig. 1a and b, respectively. In both structures, the Ba^{2+} cation is coordinated to nine O atoms with bond distances ranging from 2.719(3) to 2.952(3) Å and from 2.729(3) to 3.136(3) Å in **1** and **2**, respectively, to give the deformed coordination polyhedra shown in Fig. 2a and b. The cation coordination can be rationalized in terms of the concept of *Bond Valence* [58] which assumes that the total charge of the cation has to be saturated by Σs_i, i.e. the summation of the separate bond valence (s_i) of each coordinated atom *i*. The value of *s* can be calculated by the expression $s = \exp[(r_0 - r)/B]$

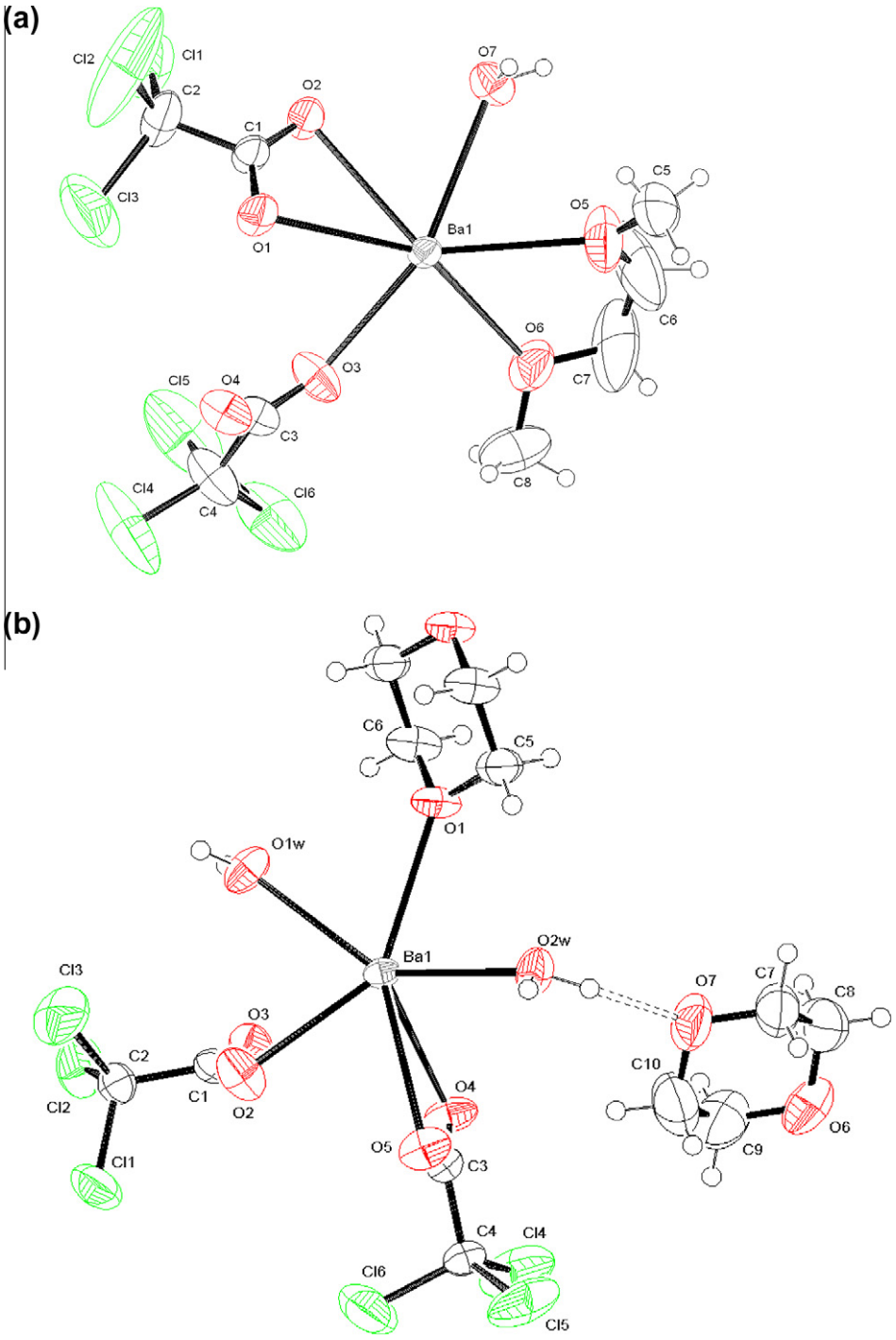

Fig. 1. ORTEP views and atom numbering scheme for **1** (a) and **2** (b). Thermal ellipsoids are drawn at the 40% probability level. Hydrogen bonds are drawn as dashed lines.

[59] where r is the actual Ba–O distances, while r_0 and B are empirical parameters with values $r_0 = 2.15998$ and $B = 0.437$ [60]. The s value obtained for the Ba^{2+} cation is 1.99 in **1** and 1.93 in **2**.

In both structures, the oxygens of the trichloroacetate ligand bridge two adjacent Ba cations, giving rise to infinite polymers. In **1**, the polymeric chains run along the *c* direction and the coordinated water molecule does not form hydrogen bonds. In **2**, the polymeric chains are extended along the *a* direction and are linked by the coordinated dioxane ligands to form a two dimensional network in the *ab* plane. The free dioxane molecules are located between these planes, linking them by the formation of O–H···O hydrogen bonds whose structural parameters are listed in Table 3. The final packing patterns for **1** and **2** are shown in Fig. 3a and b, respectively.

To compare the present crystal architectures with those exhibited by similar molecules, searches in the Cambridge Structural Database have been made of crystals containing alkaline earth metals/acetate (16 hits), alkaline earth metals/haloacetate (15 hits) and Ba/COO^- (140 hits) fragments, with the exclusion of entries in which Mg and transition metals are present. The formation of polymers turns out to be a very common situation for all alkaline earth metal, mainly due to the ability of the COO^- group to bridge adjacent metal atoms. In crystals, simple chains are found in the majority of cases with monocarboxylate ligands, giving origin to packing patterns similar to the one in Fig. 3a; as an example, the cell content for DEGJUV [61] is shown in Fig. 4a. In the case of polycarboxylate ligands, such as, for instance, oxalate, the chains are linked to give

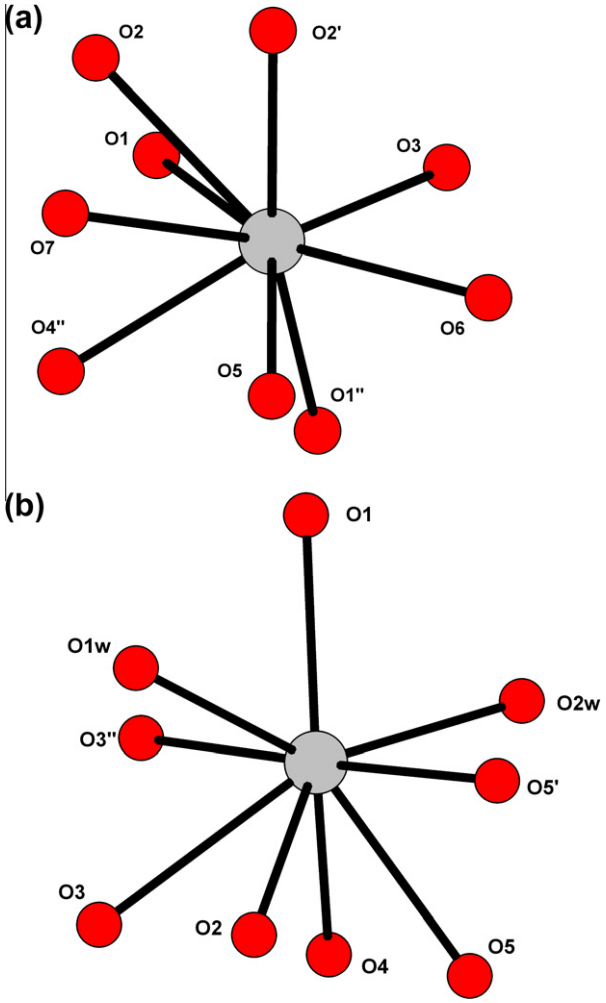

Fig. 2. Coordination around the Ba cation in compound **1** (a). Symmetry operations: O2′ (−*x*, *y*, 1/2 − *z*); O1″, O4″: (−*x*, −*y*, −*z*); compound **2** (b). Symmetry operations: O5′ (−*x*, 1 − *y*, −*z*); O3″: (1 − *x*, 1 − *y*, −*z*).

Table 3
Hydrogen bonding parameters for compound **2** (Å, °).

	D–H	D···A	H···A	D–H···A
O2W–H4W···O7	0.92	2.840(4)	2.00	150
O1W–H1W···O4^{i}	0.86(6)	2.830(5)	1.99(5)	163(4)
O1W–H2W···O6^{ii}	0.84(3)	2.881(5)	2.14(5)	146(2)
O2W–H3W···O2^{iii}	0.86	2.775(4)	2.00	148

Symmetry codes: (i) 1 − *x*, 1 − *y*, −*z*; (ii) *x*, *y*, *z* − 1; (iii) −*x*, 1 − *y*, −*z*.

planes or 3-D networks, as shown in Fig. 4b for BAOXAL02 [62]. On the contrary, the presence of cumbersome ligands prevents any aggregations, the complexes existing therefore as discrete entities as shown in Fig. 4c [63].

3.5. Thermogravimetric analysis

TGA was employed to follow the thermal behavior of the compounds and to determine various kinetic parameters of thermal decomposition, such as activation energy (E), frequency factor (A), enthalpy (ΔH), Gibbs free energy (ΔG), entropy (ΔS) etc.

3.5.1. Thermal behavior

The thermal behavior of both samples has been evaluated and representative TG/DSC superimposed curves for one of the samples, compound **2**, is shown in Fig. 5. The TG/DTG/DSC superimposed curves for compound **1** indicate that the decomposition process takes place as a multistep process:

$$Ba(H_2O)(DME)(O_2CCCl_3)_2 \rightarrow Ba(DME)(O_2CCCl_3)_2 + H_2O$$

$$Ba(DME)(O_2CCCl_3)_2 \rightarrow Ba(O_2CCCl_3)_2 + DME$$

$$Ba(O_2CCCl_3)_2 \rightarrow BaCl_2 + CCl_3COCl + CO + CO_2$$

Primarily, three major mass loss regions have been observed: the first region is associated with breakdown of the compound and release of one water molecule. The subsequent steps involve the loss of DME and finally the decomposition of $Ba(O_2CCCl_3)_2$ to barium chloride as the final product. The proposed decomposition of $Ba(O_2CCCl_3)_2$ to $BaCl_2$ as a residue and CCl_3COCl, CO, CO_2 as volatiles is similar to the reported [64] decomposition of $Cu(O_2CCCl_3)_2$ {$CuCl_2$, CCl_3COCl, CO, CO_2} and certain other metal trichloroacetates [65]. The TG results obtained experimentally are in good agreement with the calculated values, as summarized in Table 4. Transition temperatures are indicated by the DTG curves (not shown in Fig. 5 for the sake of clarity). The total observed weight loss of 63.13% in **1** and 66.55% in **2** is in excellent agreement with the calculated weight loss of 63.46% in **1** and 66.99% in **2**, for the formation of $BaCl_2$ as the final residue. For compound **2**, again a multistep decomposition takes place in a similar fashion, the first step being the removal of one dioxane molecule. In the following steps, dioxane and water are removed, followed by decomposition of $Ba(O_2CCCl_3)_2$. Barium chloride remains as the final residual product.

$$\{Ba(H_2O)_2(diox)_{0.5}(O_2CCCl_3)_2\}(diox) \rightarrow Ba(H_2O)_2(diox)_{0.5}(O_2CCCl_3)_2 + (diox)$$

$$Ba(H_2O)_2(diox)_{0.5}(O_2CCCl_3)_2 \rightarrow Ba(O_2CCCl_3)_2 + 0.5(diox) + 2H_2O$$

$$Ba(O_2CCCl_3)_2 \rightarrow BaCl_2 + CCl_3COCl + CO + CO_2$$

Separate heating of compounds **1** and **2** at 290 °C under a N_2 atmosphere gave $BaCl_2$ as the final residue, as confirmed from elemental analysis. The formation of $BaCl_2$ as the final residue is supported by the observed endothermic peaks in the DSC curves in the region 940–960 °C in both **1** and **2** (Fig. 5 shows a representative TG/DSC curve of compound **2**). These peaks in the DSC curves are related to the melting point of $BaCl_2$ as the final residue (the reported melting point of $BaCl_2$ is 961 °C) [66].

The DSC curves for the compounds prepared exhibit an endothermic process initially. The area of the endothermic peak corresponds to the heat of fusion and the peak temperature corresponds to the melting point.

3.5.2. Kinetic consideration and calculation procedure

In the present study, analysis of non-isothermal data has been performed by using the approximate computational approaches due to Coats and Redfern [67], Horowitz–Metzger [68], Madhusudanan–Krishnan–Ninan [69], van Krevelen [70] and Wanjun–Yuwen–Hen–Cunxin [71]. Integral methods are often more reliable and are generally preferred to the imprecise differential methods of kinetic analysis.

In the Coats–Redfern method, the equation has been written in the form:

$$-\ln\frac{g(\alpha)}{T^2} = -\ln\frac{AR}{\beta E}\left[1-\frac{2RT}{E}\right] + \frac{E}{RT}$$

$$\log\left[\frac{1-(1-\alpha)^{1-n}}{T^2(1-n)}\right] = \log\frac{AR}{\beta E}\left[1-\frac{2RT}{E}\right] - \frac{E}{2.303RT} \quad \text{for} \quad n\neq 1$$

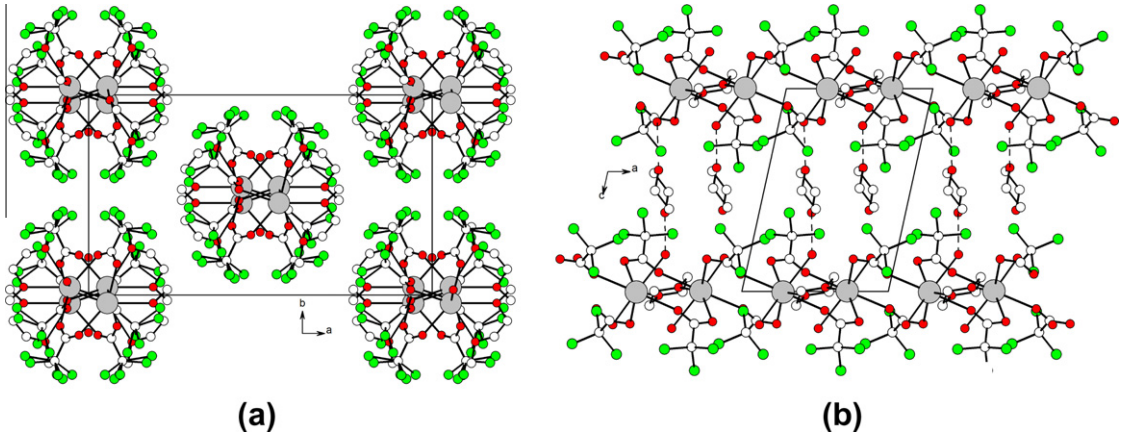

Fig. 3. Packing architectures for (a) **1** and (b) **2**. For the sake of clarity, hydrogen atoms have been omitted.

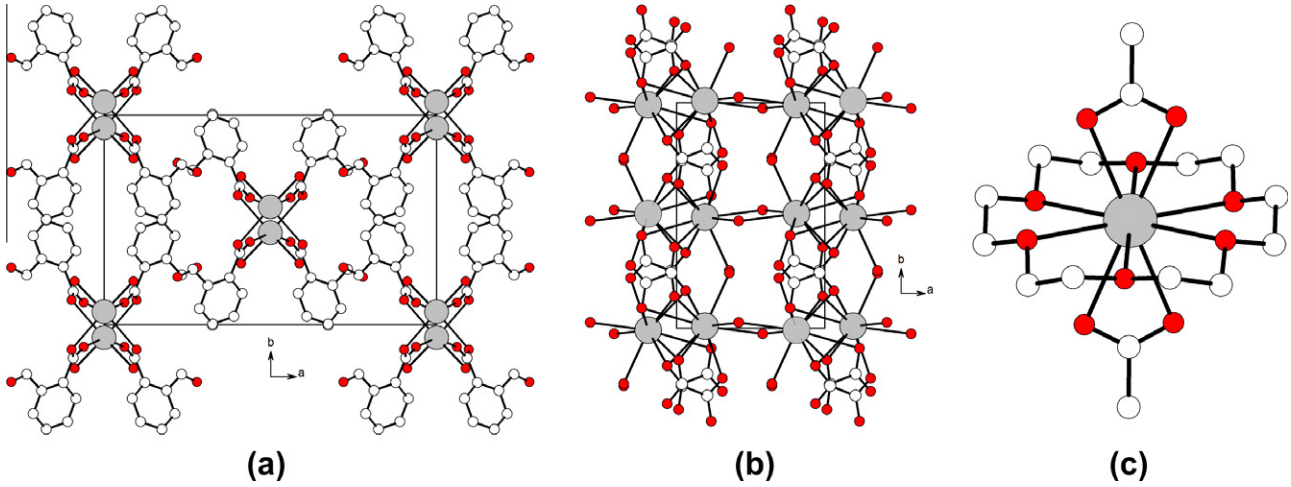

Fig. 4. (a) Cell content for DEGJUV; (b) cell content for BAOXAL02 and (c) atomic arrangement around the Ba atom in BIWBAK. For the sake of clarity, hydrogen atoms have been omitted.

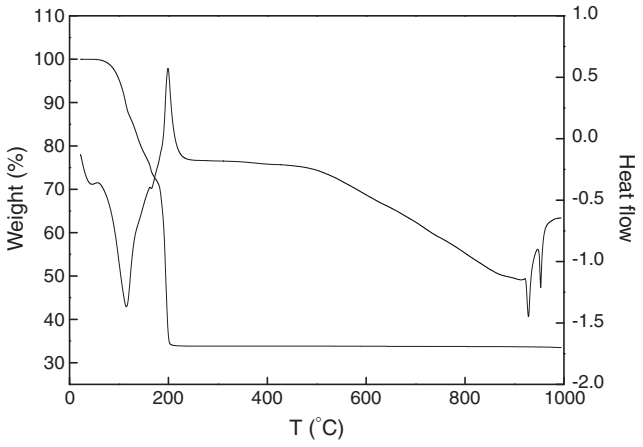

Fig. 5. Representative TG/DSC superimposed curves of sample **2** at 10 °C min^{-1}.

$$\log\left[\frac{-\log(1-\alpha)}{T^2}\right] = \log\frac{AR}{\beta E}\left[1-\frac{2RT}{E}\right] - \frac{E}{2.303RT} \quad \text{for} \quad n = 1$$

where is A is the Arrhenius constant, β the heating rate in °C min^{-1}, α the fraction of mass loss, R the gas constant, E the activation energy, n the order of the reaction and T is the temperature in K. A graphical representation of the left hand side of the above equations against $1/T$ gives a straight line with an inclination of $-2.303E/R$ and the intercept yields the value of A. In the Madhusudanan method, the equation used has the form:

$$-\ln\frac{g(\alpha)}{T^{1.9206}} = -\ln\frac{AR}{\beta E} + 3.7678 - 1.9206\ln E - 0.12040\frac{E}{RT}$$

where the symbols have their usual significance, as described above. Similar equations were obtained using methods of Wanjun–Yuwen–Hen–Cunxin and van Krevelen with different approximations. For the Wanjun–Yuwen–Hen–Cunxin method

Table 4
TGA analysis for different decomposition steps of compounds **1** and **2**.

Compound	Transition temperature (°C)	Weight loss (%)	
		Calculated	Observed
DME (**1**)	87.64	3.15	2.81
	164.95	15.78	17.17
	198.27	44.53	43.20
Dioxane (**2**)	111.90	13.97	12.94
	162.82	12.70	12.98
	193.74	40.32	40.63

Table 5
Calculation of activation energy using different methods.

Compound	Horowitz–Metzger	Coats–Redfern	Madhusudanan–Krishnan–Ninan	Wanjun–Yuwen–Hen–Cunxin	van Krevelen
	E (kJ/mol)				
1	169.708	161.587	161.890	161.591	165.714
2	149.555	140.564	140.872	140.596	145.103

Table 6
Thermodynamic decomposition parameters for compounds **1** and **2**.

Compound	E (kJ/mol)	A (min^{-1})	ΔG (kJ/mol)	ΔH (kJ/mol)	ΔS (J/mol/K)
1	161.587	1.25×10^{18}	120.82	157.69	78.61
2	140.564	7.35×10^{15}	119.82	136.66	35.90

$$-\ln\frac{g(\alpha)}{T^{1.8946}} = -\ln\frac{AR}{\beta E} + 3.6350 - 1.8946\ln E - 1.0014\frac{E}{RT}$$

and for the van Krevelen method

$$\ln g(\alpha) = \ln\left(\frac{A(0.368/T_m)^{\frac{E}{RT_m}}}{\beta\left(\frac{E}{RT_m}+1\right)}\right) + \left(\frac{E}{RT_m}+1\right)\ln T$$

In Horowitz–Metzger method, the expression is:

$$\ln\ln g(\alpha) = \frac{E\Theta}{RT_m^2}$$

where T_m is the peak temperature. The thermodynamic results of the TG and DTG evaluations employing different methods for the compounds synthesized are presented in Table 5. The results indicate that the values of all the methods are comparable and the thermodynamic data obtained by different methods agree with each other.

The various thermodynamic parameters of decomposition ΔH, enthalpy, ΔS, entropy and ΔG, Gibbs free energy of the compounds can be calculated using the following equations once E has been determined

$$\Delta S = 2.303\log\left(\frac{Ah}{kT}\right)R$$

$$\Delta H = E - RT$$

$$\Delta G = H - T\Delta S$$

where h is the Planck constant, T is the temperature in K, A is the Arrhenius constant or frequency factor, R is the gas constant and k represents the Boltzmann constant.

The result of the TG and DTG evaluations for the thermodynamic parameters are presented in Table 6. Interestingly, both compounds **1** and **2** gave the same residue, i.e. $BaCl_2$, though the decomposition mechanism followed for **1** and **2** is different. It can be seen from Tables 5 and 6 that the activation energy required for decomposition of **1** is more compared to that for **2**. The reason for this could be found in the fact that in **1** the decomposition proceeds by liberation of a water molecule which is in the inner coordination sphere, while in complex **2** the decomposition occurs by release of a dioxane molecule which is present in the outer coordination sphere. The energy of molecules bonded in the inner coordination sphere is higher than that of those bonded in the outer coordination sphere, hence it requires more energy, as is evident from the thermal calculations. Rzaczynska et al. [72] have made similar observations for 2,3-naphthalenedicarboxylates of rare earth elements, which decompose showing that the energy of the coordinated water molecules is higher than that of hydrogen bonded water molecules in the second coordination sphere.

4. Conclusion

The present synthesis has resulted in the isolation of two new polymeric barium(II) trichloroacetate compounds **1** and **2**. FT-IR studies reveal bridging trichloroacetate groups in these compounds. Compounds **1** and **2** provide new examples of barium coordinated to nine oxygen atoms in polymeric chains. These compounds thus may be explored as potential precursors in advanced material applications because of the preferential decomposition of **1** and **2** into $BaCl_2$.

Acknowledgements

Ms. Deepika Saini gratefully acknowledges the meritorious fellowship as a financial assistance from U.G.C., New Delhi, India.

Appendix A. Supplementary data

CCDC 819381 and 819382 contain the supplementary crystallographic data for **1** and **2**. These data can be obtained free of charge via http://www.ccdc.cam.ac.uk/conts/retrieving.html, or from the Cambridge Crystallographic Data Centre, 12 Union Road, Cambridge CB2 1EZ, UK; fax: (+44) 1223-336-033; or e-mail: deposit@ccdc.cam.ac.uk.

References

[1] S.R. Seidel, P.J. Stang, Acc. Chem. Res. 35 (2002) 972.
[2] M.D. Ward, J.A. McCleverty, J.C. Jeffery, Coord. Chem. Rev. 222 (2001) 251.
[3] H.A. Burkill, R. Vilar, A.J.P. White, D.J. Williams, J. Chem. Soc., Dalton Trans. (2002) 837.
[4] K.M. Fromm, E.D. Gueneau, A.Y. Robin, W. Maudez, J. Sague, R. Bergougnant, Z. Anorg. Allg. Chem. 631 (2005) 1725.
[5] S. Fujihara, Y. Kishika, T. Kimura, J. Solid State Chem. 177 (2004) 1032.
[6] T.J. Boyle, H.D. Pratt III, T.M. Alam, M.A. Rodriguez, P.G. Clem, Polyhedron 26 (2007) 5095.
[7] J. Zhang, L.G. Hubert-Pfalzgraf, D. Luneau, Polyhedron 24 (2005) 1185.
[8] B. Samanta, J. Chakroborty, N.K. Kalan, R.K. Bhubon Singh, G.P.A. Yap, C. Masschuer, J. Baumgartner, S. Mitra, Struct. Chem. 17 (2006) 139.
[9] M. Gartner, R. Fischer, J. Langer, H. Gorls, D. Walther, M. Westerhausen, Inorg. Chem. 46 (2007) 5118.
[10] J.T. Dawley, P.G. Clem, T.J. Boyle, L.M. Ottley, D.L. Overmyer, M.P. Siegal, Physica C 1–2 (2004) 143.
[11] M.P. Siegal, P.G. Clem, J.T. Dawley, R.J. Ong, M.A. Rodriguez, D.L. Overmyer, Appl. Phys. Lett. 80 (2002) 2710.
[12] B.A. Hernandez-Sanchez, T.J. Boyle, C.M. Baros, L.N. Brewer, T.J. Headley, D.R. Tallant, M.A. Rodriguez, B.A. Tuttle, Chem. Mater. 19 (2007) 1459.
[13] T.J. Boyle, B.A. Hernandez-Sanchez, C.M. Baros, L. Brewer, M.A. Rodriguez, Chem. Mater. 19 (2007) 2016.
[14] F. Gschwind, A. Crochet, W. Maudez, K.M. Fromm, Chimia 64 (2010) 299.
[15] F. Gschwind, O. Sereda, K.M. Fromm, Inorg. Chem. 48 (2009) 10535.
[16] K.M. Fromm, Coord. Chem. Rev. 252 (2008) 856.
[17] W. Maudez, M. Meuwly, K.M. Fromm, Chem. Eur. J. 13 (2007) 8302.
[18] G.B. Deacon, P.C. Junk, G.J. Moxey, K. Ruhlandt-Senge, C. Stprox, M.F. Zungia, Chem. Eur. J. 15 (2009) 5503.
[19] J.M. Harrowfield, W.R. Richmond, B.W. Skelton, A.H. White, Eur. J. Inorg. Chem. (2004) 227.
[20] Z. Quan, D. Yang, P. Yang, X. Zhang, H. Lian, X. Liu, J. Lin, Inorg. Chem. 47 (2008) 9509.
[21] Y. Yang, G. Jiang, Y.-Z. Li, J. Bai, Y. Pan, X.-Z. You, Inorg. Chim. Acta 359 (2006) 3257.

[22] K.F. Tesh, D.J. Burkley, T.P. Hanusa, J. Am. Chem. Soc. 116 (1994) 2409.
[23] K.G. Caulton, M.H. Chisholm, S.R. Drake, K. Folting, J.C. Huffman, W.E. Streib, Inorg. Chem. 32 (1993) 1970.
[24] W.A. Herrmann, N.W. Huber, O. Runte, Angew. Chem., Int. Ed. Engl. 34 (1995) 2187.
[25] S.R. Drake, M.B. Hursthouse, K.M.A. Malik, S.A.S. Miller, J. Chem. Soc., Chem. Commun. (1993) 478.
[26] J.A. Darr, S.R. Drake, M.B. Hursthouse, K.M.A. Malik, S.A.S. Miller, D.M.P. Mingos, J. Chem. Soc., Dalton Trans. (1997) 945.
[27] V.-C. Arunasalam, I. Baxter, S.R. Drake, M.B. Hursthouse, K.M.A. Malik, S.A.S. Miller, D.M.P. Mingos, D.J. Otway, J. Chem. Soc., Dalton Trans. (1997) 1331.
[28] K.D. Pollard, J.J. Vittal, G.P.A. Yap, R.J. Puddephatt, J. Chem. Soc., Dalton Trans. (1998) 1265.
[29] D.C. Bradley, Chem. Rev. 89 (1989) 1317.
[30] D.C. Bradley, R.C. Mehrotra, I.P. Rothwell, A. Singh, Alkoxo and Aryloxo Derivatives of Metals, Academic Press, New York, 2001, p. 704.
[31] C.D. Chandler, C. Roger, M.J. Hampden-Smith, Chem. Rev. 93 (1993) 1205.
[32] T.J. Boyle, S.D. Bunge, T.M. Alam, G.P. Holland, T.J. Headley, G.R. Avilucea, Inorg. Chem. 44 (2005) 1309.
[33] T.J. Boyle, S.D. Bunge, N.L. Andrews, L.E. Matzen, K. Sieg, M.A. Rodriguez, T.J. Headley, Chem. Mater. 16 (2004) 3279.
[34] T.J. Boyle, S.D. Bunge, P.G. Clem, J. Richardson, J.T. Dawley, L.A.M. Ottley, M.A. Rodriguez, B.A. Tuttle, G.R. Avilucea, R.G. Tissot, Inorg. Chem. 44 (2005) 1588.
[35] Conquest Version 1.9, Cambridge Crystallographic Data Centre, 2004, Available from: http://www.ccdc.cam.ac.uk.
[36] J. Zhao, K.H. Dahmen, H.O. Marcy, L.M. Tonge, B.W. Wessels, T.J. Marks, C.R. Kannewurf, Solid State Commun. 69 (1989) 187.
[37] G.R. Paz-Pujalt, Physica C 166 (1990) 177.
[38] T. Araki, I. Hirabayashi, Supercond. Sci. Technol. 16 (2003) R71.
[39] T. Araki, I. Hirabayashi, T. Niwa, Supercond. Sci. Technol. 17 (2004) 135.
[40] S. Mishra, J. Zhang, L.G. Hubert-Pfalzgraf, D. Luneau, E. Jeanneau, Eur. J. Inorg. Chem. (2007) 602.
[41] D. Prodius, C. Turta, V. Mereacre, S. Shova, M. Gdaniec, Y. Simonov, J. Lipkowski, V. Kuncser, G. Filoti, A. Caneschi, Polyhedron 25 (2006) 2175.
[42] C. Turta, S. Shova, D. Prodius, V. Mereacre, M. Gdaniec, Y. Simonov, J. Lipkowski, Inorg. Chim. Acta 357 (2004) 4396.
[43] A.I. Vogel, A Text Book of Quantitative Inorganic Analysis, fourth ed., Longmans, London, 1978.
[44] Z. Otwinowski, Z. Minor, in: C.W. Carter, R.M. Sweet (Eds.), Methods in Enzymology, vol. 276 Part A, Academic Press, London, 1977, pp. 307–326.
[45] R.H. Blessing, Acta Crystallogr., Sect. A 51 (1995) 33.
[46] A. Altomare, M.C. Burla, M. Camalli, G.L. Cascarano, C. Giacovazzo, A. Guagliardi, A.G. Moliterni, G. Polidori, R. Spagna, J. Appl. Crystallogr. 32 (1999) 115.
[47] G.M. Sheldrick, SHELXL97, Program for Crystal Structure Refinement, University of Göttingen, Göttingen, Germany, 1997.
[48] L.J. Farrugia, J. Appl. Crystallogr. 32 (1999) 837.
[49] K. Starke, J. Inorg. Nucl. Chem. 26 (1964) 1125.
[50] A.V.R. Warrier, R.S. Krishnan, Spectrochim. Acta 27A (1971) 1243.
[51] A.B.P. Lever, D. Ogden, J. Chem. Soc. (A) (1967) 2041.
[52] D.B. Dell'Amico, R. Alessio, F. Calderazzo, F.D. Pina, U. Englert, G. Pampaloni, V. Passarelli, J. Chem. Soc., Dalton Trans. (2000) 2067.
[53] J. Powell, T. Jack, Inorg. Chem. 11 (1972) 1039.
[54] R.C. Mehrotra, R. Bohra, Metal Carboxylates, Academic Press, London, UK, 1983.
[55] G.B. Deacon, R.J. Philips, Coord. Chem. Rev. 33 (1980) 227.
[56] W.J. Geary, Coord. Chem. Rev. 7 (1971) 81.
[57] M.N. Burnett, C.K. Johnson, ORTEP-III: Oak Ridge Thermal Ellipsoid Plot Program for Crystal Structure Illustrations, Report ORNL-6895, Oak Ridge National Laboratory, Oak Ridge, TN, 1996.
[58] I.D. Brown, Chem. Soc. Rev. 7 (1978) 359.
[59] I.D. Brown, D. Altermatt, Acta Crystallogr. B41 (1985) 244.
[60] S. Adams, Acta Crystallogr. B57 (2001) 278.
[61] M. Odabasoglu, O. Buyukgungor, Acta Crystallogr., Sect. E 62 (2006) m402.
[62] A.N. Christensen, R.G. Hazell, A.M.T. Bell, A. Altomare, J. Phys. Chem. Solids 56 (1995) 1359.
[63] L. Archer, M.J. Hampden-Smith, E. Duesler, Polyhedron 17 (1998) 713.
[64] M.D. Judd, B.A. Plunkett, M.I. Pope, J. Therm. Anal. 9 (1976) 83.
[65] G.P. Tilloy, J.E. Roberts, Inorg. Chem. 2 (1963) 745.
[66] D.R. Lide, CRC Handbook of Chemistry and Physics, 89th ed., CRC Press, New York, 2008–09.
[67] A.W. Coats, J.P. Redfern, Nature 201 (1964) 68.
[68] H.H. Horowitz, G. Metzger, Anal. Chem. 35 (1963) 1464.
[69] P.M. Madhusudanan, K. Krishnan, K.N. Ninan, Thermochim. Acta 22 (1993) 13.
[70] D.W. van Krevelen, C. Van Heerden, F.J. Huntjens, Fuel 30 (1951) 253.
[71] T. Wanjun, L. Yuwen, Z. Hen, W. Cunxin, J. Therm. Anal. Cal. 74 (2003) 309.
[72] Z. Rzaczynska, A. Kula, J. Sienkiewicz-Gromiuk, A. Szybiak, J. Therm. Anal. Calorim. 103 (2011) 275.